FLAME EXTINGUISHMENT IN A CUP-BURNER APPARATUS

Fumiaki Takahashi*
National Center for Microgravity Research on Fluids and Combustion
NASA Glenn Research Center
Cleveland, Ohio 44135

Gregory T. Linteris
Fire Research Division, National Institute of Standards and Technology
Gaithersburg, MD 20899

Viswanath R. Katta
Innovative Scientific Solutions, Inc.
Dayton, Ohio 45440

Abstract

Unsteady extinguishment phenomena of laminar methane-air co-flow diffusion flames formed in a cup-burner apparatus at normal earth gravity have been studied experimentally and computationally. A gaseous fire-extinguishing agent (CO_2, N_2, He, Ar, or CF_3H) was introduced gradually into a coflowing oxidizer stream until blowoff-type extinguishment occurred. The agent concentration in the oxidizer required for extinguishment was nearly independent of a wide range of the mean oxidizer velocity, exhibiting a so-called plateau region, for all agents except helium. Numerical simulations with detailed chemistry were performed to reveal the detailed flame structure and to predict the minimum extinguishing concentration (MEC) of agent at a fixed oxidizer velocity for a comparison with the experiment previously conducted. The MEC values of agents determined were: experiment: CF_3H, (11.7 ± 0.8) %; CO_2, (15.7 ± 0.6) %; N_2, (25.9 ± 1.0) %; He, (26.7 ± 1.1) %; and Ar, (37.3 ± 1.5) %; computation: CF_3H, 10.1 %; CO_2, 14.5 % (or 16.1 % with different kinetic parameters for a methyl-H atom reaction step); N_2, 25.2 %; He, ~23 %; and Ar, 35.7 %. Despite the complexity of chemistry and flame-flow interactions in the blowoff processes, the numerical predictions of MECs were generally in good agreements (~6% less, on average) with the measurements. The relative ranking of the MECs depended upon primarily a reverse order of the heat capacity of the agent-laden oxidizers for all of the inert agents tested.

Introduction

The effectiveness of gaseous fire-extinguishing agents, typically used in total flooding fire suppression systems, depends on the agents' ability to extinguish a fire at the lowest possible concentrations. To determine the effectiveness of gaseous fire-extinguishing agents, the cup burner method, specified in national and international standards [1,2], has most widely been used [3-10] in terrestrial fire safety engineering. The cup-burner flame is a laminar co-flow diffusion flame with a circular fuel source (either a liquid pool or a low-velocity gas jet) inside a co-axial chimney with an oxidizing stream. An agent is generally introduced into the coflowing oxidizer in the cup-burner apparatus to determine the minimum extinguishing concentration (MEC) of agent. The MEC measured by the cup burner is then used for determining the minimum design concentration of a gaseous agent by adding a margin to the MEC value and third-party approval procedures for a complete fire extinguishing system [10].

The cup-burner flame resembles a real fire, which consists of flame segments subjected to various strain rates and exhibits flame flickering (and separation) in normal earth gravity, affecting the air and agent entrainment into the flame zone. Moreover, a real fire over condensed materials generally forms a leading flame edge, which plays an important role in flame stabilization, spreading, and suppression. Thus, the cup burner flame serves as a scale model of real fires for evaluating the agent effectiveness. Because of its resemblance to fires, great faith has been placed in the cup-burner MEC values, and many safety codes and design practices are based on them. However, fundamental understanding of the flame extinguishment processes for this device is very limited. Little is known concerning the amount of agent that is transported into various regions of the flame, or whether the extinguishment occurs due to global flame extinction or destabilization of the edge diffusion flame. Clearly, the understanding of fire suppression by chemical inhibitors as well as inert-gas agents would be greatly improved if their

* Corresponding author: Fumiaki.Takahashi@grc.nasa.gov
Proceedings of the Fourth Joint Meeting of the U.S. Sections of The Combustion Institute, March 21-23, 2005.

effect in cup-burner flames was investigated from a fundamental perspective.

It is well known that fire suppressants work through their physical and/or chemical action [5, 11]. By using physically acting inert gases (N_2, Ar, and CO_2) and their mixtures, Senecal [10] has developed an explicit relationship for cup-burner extinguishing concentration in terms of (products and agent) heat capacity and fuel (n-heptane) properties. As a result of significant progresses in the development of detailed combustion reaction mechanisms and computational methodologies over the last decade or two, it is now feasible to simulate various transient combustion phenomena in simple configurations (burner geometry, flow, and fuel) with confidence, leading to deeper understanding of physical and chemical processes taking place during the phenomena under investigation. In recent years, the authors have investigated [12-20] the diffusion flame structure, blowoff phenomena, and physical and chemical suppression processes. Major findings include a decisive role of the peak reactivity spot (i.e., *reaction kernel*), formed at the flame attachment point in the edge diffusion flame, in blowoff processes.

The overall objectives of the present study are to understand the physical and chemical processes of cup-burner flame extinguishment and to provide rigorous testing of numerical models, which include detailed chemistry and radiation sub-models. This paper reports the calculated flame structure changes in response to various inert-gas agents and compares the predicted extinguishment limits with the previously measured MECs.

Experimental Procedures

The cup burner, described previously [7], consists of a cylindrical glass cup (28 mm inner diameter, 31 mm outer diameter, 45º-chamfered inside burner rim) positioned inside a glass chimney (8.5 cm or 9.5 cm inner diameter, 53.3 cm height). To provide uniform flow, 6 mm glass beads fill the base of the chimney, and 3 mm glass beads (with two 15.8 mesh/cm screens on top) fill the fuel cup. Gas flows were measured by mass flow controllers (Sierra 860*) which were calibrated so that their uncertainty is 2 % of indicated flow. The burner rim temperature, measured at 3.7 mm below the exit using a surface temperature probe after running the burner for ≈10 minutes, was (514 ± 10) K.

The fuel gas used is methane (Matheson UHP, 99.9 %), and the agents are carbon dioxide (Airgas, 99.5 %), nitrogen (boil-off), helium (MG Ind., 99.95 %), and argon (MG Ind., 99.996 %). The air is house compressed air (filtered and dried) which is additionally cleaned by passing it through an 0.01 μm filter, a carbon filter, and a desiccant bed to remove small aerosols, organic vapors, and water vapor. To determine the suppression condition, for a fixed methane flow rate (0.34 L/min which converts to the mean fuel velocity of 0.92 cm/s), the agent was added (in increments of < 1 % near extinguishment) to co-flowing air (held at a constant flow rate) until extinguishment occurred. The test was repeated at least three times at each of the different coflow velocities.

An uncertainty analysis was performed, consisting of calculation of individual uncertainty components and root mean square summation of components. All uncertainties are reported as *expanded uncertainties*: $X \pm ku_c$, from a combined standard uncertainty (estimated standard deviation) u_c, and a coverage factor $k = 2$. Likewise, when reported, the relative uncertainty is ku_c/X. The expanded relative uncertainties for the experimentally determined quantities in this study are 4 % for the volume fractions of CO_2, N_2, He, and Ar.

Computational Methods

A time-dependent, axisymmetric numerical code (UNICORN) [21] is used for the simulation of unsteady co-flowing diffusion flames stabilized on the cup burner. The code solves the axial and radial (z and r) full Navier-Stokes momentum equations, continuity, and enthalpy- and species-conservation equations on a staggered-grid system. The body-force term due to the gravitational field is included in the axial-momentum equation to simulate upward-oriented flames. A clustered mesh system is employed to trace the gradients in flow variables near the flame surface. A detailed reaction mechanism of GRI-V1.2 [22] for methane-oxygen combustion (31 species and 346 elementary reactions) and NIST CKMech [23] for fluoromethane inhibition reactions (82 species and 1510 elementary reactions) (for CF_3H agent only) are incorporated into UNICORN. Thermophysical properties of species are calculated from the polynomial curve fits for 300 - 5000 K. Mixture viscosity and thermal conductivity are then estimated using the Wilke and Kee expressions, respectively. A simple radiative heat-loss model [24] based on optically thin-media assumption and Plank-mean absorption coefficients for CO_2, H_2O, CH_4, and CO, was incorporated into the energy equation.

The finite-difference forms of the momentum equations are obtained using an implicit QUICKEST scheme [25], and those of the species and energy equations are obtained using a hybrid scheme of upwind and central differencing. At every time-step, the pressure field is accurately calculated by solving all the pressure Poisson equations simultaneously and using the LU (Lower and Upper diagonal) matrix-decomposition technique.

Unsteady axisymmetric calculations for the cup-burner flames are made on a physical domain of 200 mm by 47.5 mm using a 251 × 101 or 541 × 251 non-uniform grid system that yielded 0.2 mm by 0.2 mm or 0.05 mm by 0.05 mm minimum grid spacing, respectively, in both the z and r directions in the flame zone. The computational domain is bounded by the axis of symmetry and a chimney wall boundary in the radial direction and by the inflow and outflow boundaries in the axial direction. The boundary conditions are treated in the same way as those reported in earlier papers [14-20]. The outflow boundary in z direction is located sufficiently far from the burner exit (>7 fuel-cup diameters) such that propagation of

*Certain commercial equipment, instruments, or materials are identified in this paper to adequately specify the procedure. Such identification does not imply recommendation or endorsement by NIST or NASA, nor does it imply that the materials or equipment are necessarily the best available for the intended use.

boundary-induced disturbances into the region of interest is minimal. Flat velocity profiles are imposed at the fuel and air inflow boundaries, while an extrapolation procedure with weighted zero- and first-order terms is used to estimate the flow variables at the outflow boundary.

The inner diameter of the cup burner is 28 mm and the burner wall is treated as a 1-mm long and 1-mm thick tube. The wall temperature is set at 600 K, which is somewhat higher than the afore-mentioned measurement made below the exit. The chimney inner diameter is 95 mm. The mean fuel and oxidizer velocities are 0.921 cm/s and 10.7 cm/s, respectively. The low fuel velocity represents a condition at which the flame size is comparable to that of typical liquid-fuel cup-burner flames. The air velocity is in the middle of the so-called "plateau region" [1, 6, 8], where the extinguishing agent concentration is independent of the oxidizer velocity.

Results and Discussion

Minimum Extinguishing Concentrations

Figure 1 shows the measured and calculated critical agent volume fractions in the oxidizer at extinguishment ($X_{a,exp}$, $X_{a,cal}$, respectively), or minimum extinguishing concentrations (MEC), for various fire-extinguishing agents. The results for CO_2 and CF_3H have been reported in detail elsewhere [14, 17-20]. The measured critical agent volume fractions were nearly independent of the mean oxidizer velocity (U_{ox}) over wide ranges tested for all agents except He, for which $X_{a,exp}$ decreased mildly with increasing U_{ox}. The insensitivity of the extinguishment limit to the oxidizer flow (plateau region), once a minimum flow is achieved, has been reported in the literature [1, 6, 8]. The fuel velocity, fuel-cup diameter, and chimney diameter are also known to have a small or negligible impact on the agent concentration at suppression [6].

In the plateau region for CO_2, the data points obtained using the standard glass burner (□) were consistent with those obtained with the stainless-steel burner (○) with a sufficient preheating period [20]. As the oxidizer velocity was decreased below the lower edge of the plateau region and approached a threshold ($U_{ox} \approx 1$ cm/s) for forming an over-ventilated flame, $X_{a,exp}$ decreased rapidly toward zero. Thus, an under-ventilated flame in $U_{ox} < 1$ cm/s could never been stabilized on the burner.

Table 1 lists the measured and calculated critical agent volume fractions at extinguishment (or MECs), the corresponding limiting oxygen volume fractions ($X_{O2,exp}$, $X_{O2,cal}$), the heat capacity of the oxidizer at 298 K ($C_{p,ox}$), and the adiabatic flame temperature (T_f) [26] of the stoichiometric methane-air mixture at the measured extinguishing condition for various agents. The limiting oxygen volume fraction was converted from the extinguishing agent volume fraction as $X_{O2} = X_{O2,initial}(1 - X_a)$, where $X_{O2,initial}$ = the initial oxygen volume fraction in the neat oxidizer.

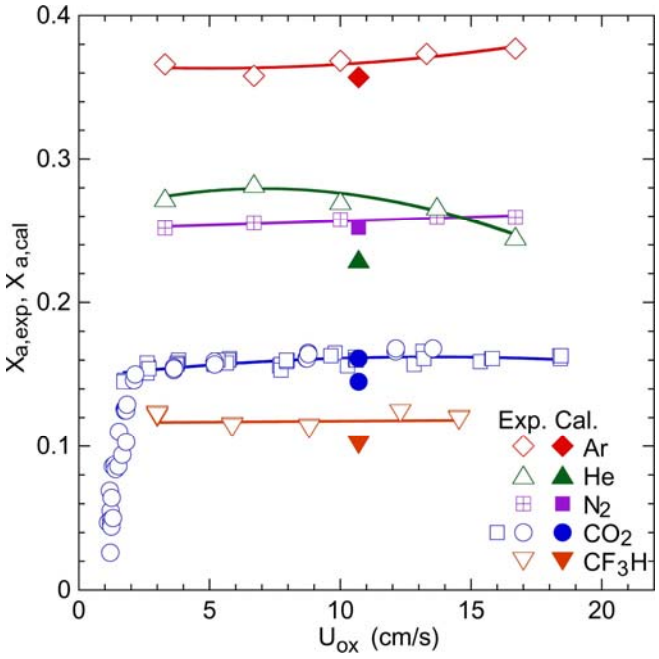

Fig. 1 Measured and calculated critical agent volume fractions at extinguishment.

The MEC value for CF_3H was the lowest (most effective) and that for Ar was highest (least effective). The predicted MEC values at a fixed oxidizer velocity (U_{ox} = 10.7 cm/s) were ~6%, on average, less than the measured values. Considering the complexity of the chemical reaction mechanism as well as the dynamic flame-flow interactions in blowoff processes leading to extinguishment, the predictions are in good agreement with measurements. The high coefficient of determination (R^2 = 0.98) for the linear correlation indicates consistency in the predictions for various agents, including CF_3H. As reported previously [16], the use of different kinetic parameters [27] for the methyl-H atom

Table 1 Extinguishment limit, heat capacity, and adiabatic flame temperature.

Agent	$X_{a,exp}$	$X_{a,cal}$	$X_{O2,exp}$	$X_{O2,cal}$	$\frac{(X_{ac,cal} - X_{ac,exp})}{X_{ac,exp}}$	$C_{p,ox}$ at $X_{a,exp}$ (J/mol K)	T_f (K) at $X_{a,exp}$
CF_3H	0.117 ± 0.008	0.101	0.185 ± 0.002	0.189	-0.137	31.85	2109
CO_2	0.157 ± 0.006	0.145 0.161[a]	0.177 ± 0.001	0.180 0.176[a]	-0.076 0.025	30.43	1927
N_2	0.259 ± 0.01	0.252	0.155 ± 0.002	0.157	-0.027	29.16	1900
He	0.267 ± 0.011	~0.23	0.154 ± 0.002	0.162	-0.139	26.94	2001
Ar	0.373 ± 0.015	0.357	0.131 ± 0.003	0.135	-0.043	26.05	1875

[a] Using different kinetic parameters [27] for a methyl-H atom reaction step [16]

reaction step ($CH_3 + H + M \rightarrow CH_4 + M$) resulted in almost exact matching (●, upper data point in Fig. 1) with the measurement for CO_2. It is anticipated that this effect applies to other agents as well. The predicted MEC for He is particularly low as the computation was stopped at the point when the flame base lifted ~50 mm.

The relative ranking of the agent effectiveness:

$$CF_3H > CO_2 > N_2 \approx He > Ar,$$

is essentially that of the oxidizer heat capacity, suggesting that dilution and thermal effects prevail, even with CF_3H. To examine the relative global effects of various agents, it is useful to examine the calculated adiabatic temperature (although the actual flame temperature is substantially lower due to heat losses). Figure 2 shows the heat capacity of the oxidizer stream as well as the adiabatic flame temperature of a stoichiometric mixture of methane with the oxidizer, as a function of the agent volume fraction (X_a); the measured extinguishment conditions ($X_{a,exp}$) for various agents are shown by the points. Adding an agent has three global effects: diluting the mixture, varying the heat capacity of the mixture, and (for CF_3H) changing the heat release per unit mass of oxidizer (due to reaction of the agent itself). For N_2, there is the dilution effect only (C_p for N_2 or O_2 is about 29 J/mol K). For CO_2 and CF_3H, $C_{p,ox}$ increases (C_p for CO_2 is 37.129 J/mol K and that for CF_3H is 52.011 J/mol K), while for He and Ar, $C_{p,ox}$ decreases (C_p for He and Ar is 20.8 J/mol K). The calculated adiabatic flame temperature accounts for these two effects. For example, at the extinguishment point, adding CO_2, N_2, or Ar, reduced T_f to about 1900 K (bounded by horizontal dashed lines) as compared T_f for neat air (2223 K), whereas adding He and CF_3H yielded a higher T_f (> 2000 K), suggesting that there were some other effects as well. For example, with CF_3H, despite its much high heat capacity, T_f is actually much greater than that for N_2 (with has neutral $C_{p,ox}$ as compared to air). This result indicates that adding CF_3H increased the chemical enthalpy input into the system (i.e., fuel effect). Nonetheless, the flame was extinguished at a relatively high temperature (due to chemical inhibition by removal of chain radicals, as described in more detail elsewhere [17]).

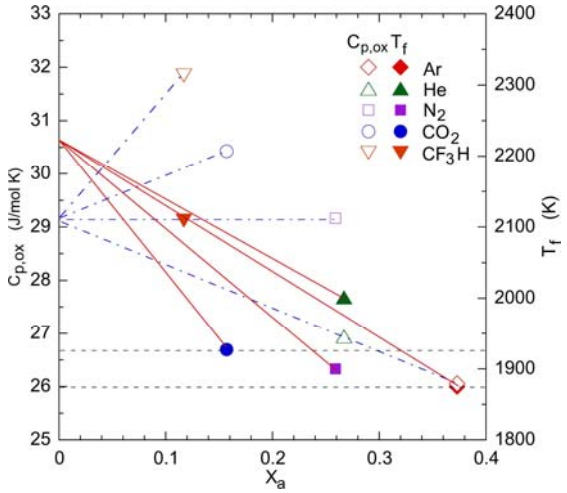

Fig. 2 Oxidizer heat capacity and adiabatic flame temperature at measured extinguishing limits.

Although the molar heat capacity of Ar and He are identical, extinguishment occurred at much lower $X_{a,exp}$ for He, probably due to premature flame destabilization. Potential causes include effects of its physical properties, particularly density, thermal conductivity, and diffusivity on the fluid dynamic and thermal structure of the flame stabilizing region. Helium decreases the density of the coflowing stream, thus reducing the buoyancy effect, and it also increases the mixture thermal diffusivity, which increases the conduction heat losses from the attachment point, but also increases the burning velocity once premixing occurs. Helium diffuses rapidly, thereby even diluting the fuel stream.

Flame Structure and Extinguishing Processes

The inner structure of the flame attachment region, revealed by the numerical simulation, provides more detailed physical and chemical insights into the extinguishment processes. It has been elucidated previously [12, 13] that the peak reactivity spot (reaction kernel) in the edge diffusion flame is responsible for the flame attachment and blowoff phenomena. Figure 3 shows the effect of agents on various reaction-kernel properties: the axial and radial stand-off distance from the outer edge of the burner rim (z_k, $y_k = r_k - 14$,

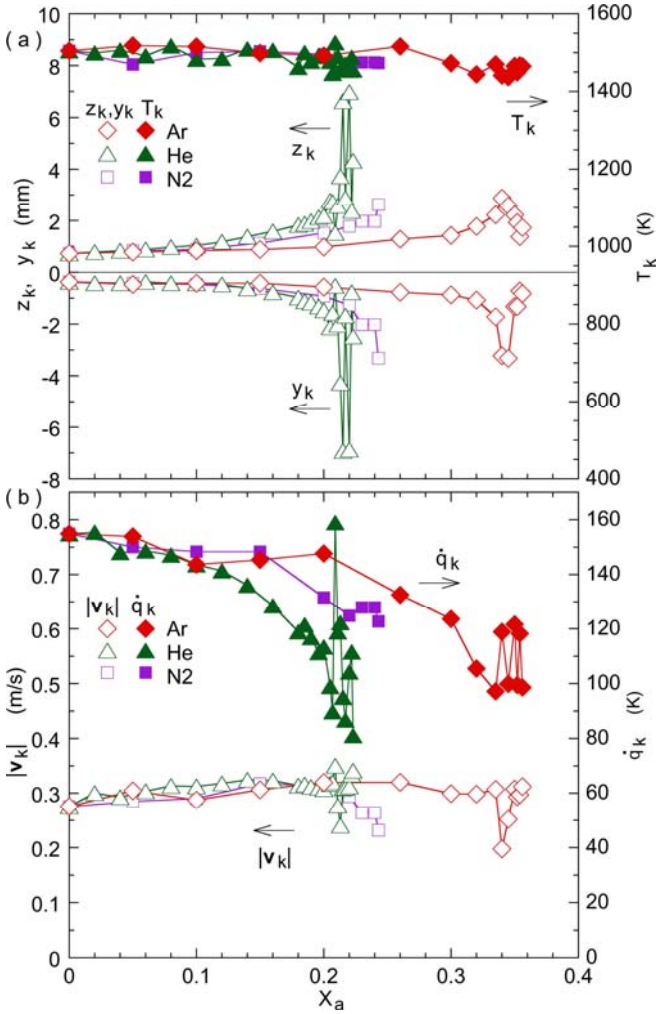

Fig. 3 Effects of agent volume fraction on the calculated reaction-kernel properties.

respectively), temperature (T_k), velocity ($|\mathbf{v}_k|$), and heat-release rate ($\dot{q}_k$), for N_2, He, and Ar. As the agent volume fraction was increased, the reaction kernel gradually moved inward (decreasing y_k) and above the burner (increasing z_k), whereas the temperature remained nearly constant (~1500 K). The velocity was also nearly constant (~0.3 m/s), whereas the heat-release rate decreased substantially due to dilution.

Figure 4 shows the calculated structure of a near-extinguishing methane flame in the air with 21.5% He added, including the velocity vectors (**v**), isotherms (T), total heat-release rate ($\dot{q}$), and the local equivalence ratio (ϕ_{local}). The local equivalence ratio is defined by considering a stoichiometric expression for intermediate species in the mixture to be converted to CO_2 and H_2O and is identical to the conventional equivalence ratio in the unburned fuel-air mixture. The velocity vectors show the longitudinal acceleration in the hot zone due to buoyancy. The heat-release rate contours showed a peak reactivity spot (reaction kernel) at the flame base. The heat-release rate, velocity, temperature, and local equivalence ratio at the reaction kernel were $\dot{q}_k$ = 95.0 J/cm^{3}s, $|v_k|$ = 0.309 m/s T_k = 1460 K, and ϕ_{local} = 0.73, respectively. The reaction kernel was still holding the much weaker trailing flame zone at higher velocities. As the fuel-air premixing progressed in the expanded quenched zone between the flame base and the burner rim, the reaction kernel could propagate back toward the rim and, thus, oscillated before extinguishment by repeating the cycle. The flame base oscillation was influenced by the flame flickering, which affected the entrainment velocity, as reported previously [18]. If the flame base propagated back to the burner rim during the oscillation cycle, the heat-release rate at the reaction kernel could exceed that for the undiluted flame (Fig. 3b). If the flame base could not propagate back and drifted away downstream, the blowoff extinguishment occurred. Thus, the cup-burner extinguishment phenomenon is neither due to global extinction of the trailing diffusion flame nor local extinction at the reaction kernel. It is rather due to continuous flame stabilization (or destabilization) processes to search a new balancing point in the flow in response to an increase in the agent concentration.

Figure 5 shows the variations of calculated variables across the reaction kernel of the flame in the air with 21.5 % He, which reduced the oxygen concentration in the oxidizer from 21 % to 16.5 %. The formation rates of species, including chain radicals (OH, H, and O), as well as the heat-release rate decreased significantly (~40 % reduction) compared with the flame in the neat air [19]. Further work is necessary to determine the reasons for helium's anomalous behavior.

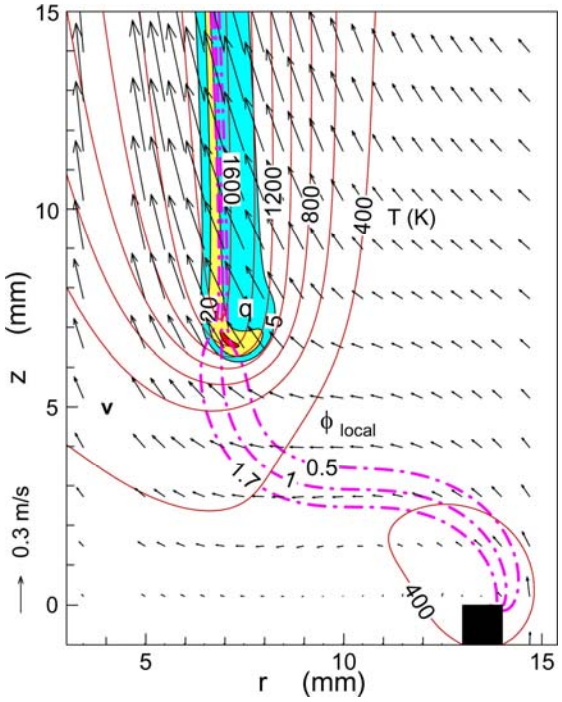

Fig. 4 Calculated structure of a methane flame in air with 21.5% added He. q contours: 5, 20, and 80 J/cm^{3}s.

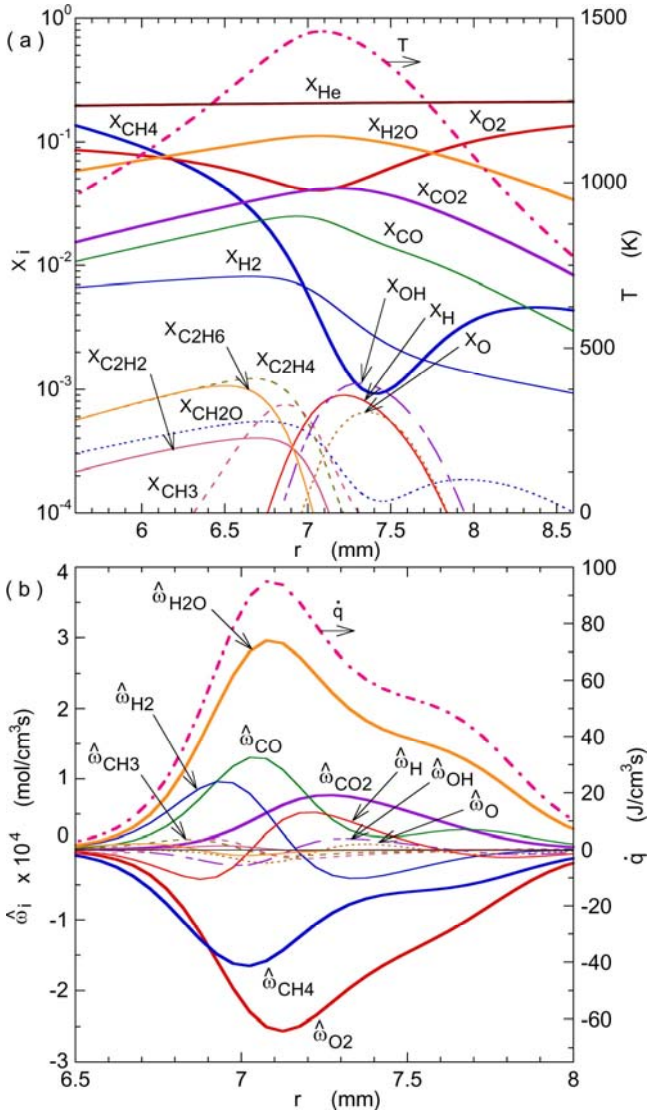

Fig. 5 Calculated variables across the reaction kernel of a methane flame in air with 21.5% added He. z_k = 6.63 mm. (a) Mole fractions, temperature, (b) production rate, and heat-release rate.

Conclusions

The numerical simulations with full chemistry have revealed the flame structure and extinguishment behavior of laminar methane diffusion flames in co-flowing air in the cup-burner configuration under normal earth gravity. By considering the complexity of the chemical reaction mechanism as well as the dynamic flame-flow interactions in blowoff processes, the predicted MEC values are in good agreement with measurements. The relative ranking of the effectiveness of agents:

$$CF_3H > CO_2 > N_2 \approx He > Ar,$$

is essentially in the order of the oxidizer heat capacity, implying that dilution and thermal effects prevail. Nonetheless, examination of the calculated adiabatic flame temperature at extinction illustrates that CF_3H reaction increases the heat release per unit mass of the reactants, so that CF_3H must also display significant chemical inhibition in order to end up acting comparably to the inert agents.

Acknowledgment

This work was supported by the Office of Biological and Physical Research, National Aeronautics and Space Administration, Washington, DC.

References

1. Annon., "Standard on Clean Agent Fire Extinguishing Systems," National Fire Protection Association, NFPA 2001, Quincy, MA, 2000.
2. Annon., "Gaseous Fire-Extinguishing Systems—Physical Properties and System Design," International Organization for Standardization, ISO 14520-Part I, 2000.
3. Bajpai, S. N., "An Investigation of the Extinction of Diffusion Flames by Halons," Journal of Fire and Flammability 5: 255 (1974).
4. Hirst, R., and Booth, K., "Measurements of Flame-Extinguishing Concentrations," Fire Technology 13: 4 (1977).
5. Sheinson, R. S., Pener-Hahn, J. E., and Indritz, D., "The Physical and Chemical Action of Fire Suppressants," Fire Safety Journal 15: 437-450 (1989).
6. Hamins, A., Gmurczyk, G., Grosshandler, W., Rehwoldt, R. G., Vazquez, I., Cleary, T., Presser, C., and Seshadri, K., "Flame Suppression Effectiveness," NIST SP 861, 1994, pp. 345-465.
7. Linteris, G.T. and Gmurczyk, GW., "Prediction of HF Formation During Suppression," NIST SP 890: Vol. II, 1995, pp. 201-318.
8. Moore, T. A., Martinez, A., and Tapscott, R. E., "A Comparison of the NMERI and ICI-style Cup-Burners," Proceedings of the 7th Halon Options Technical Working Conference (HOTWC-97), 1997, pp. 388-395.
9. Saito, N., Ogawa, Y., Saso, Y., and Sakai, R., "Improvement on Reproducibility of Flame Extinguishing Concentration Measured by Cup Burner Method," Report of Fire Research Inst. of Japan, No. 81, 1996, pp. 22-29.
10. Senecal, J. A., "Flame Extinguishing by Inert Gases: Theoretical & Experimental Analysis," Central States Section/The Combustion Institute Meeting, March 2004.
11. Williams, F.A., J. Fire Flammability, 5, 54 (1974).
12. Takahashi, F., Schmoll, W. J., and Katta, V. R., "Attachment Mechanisms of Diffusion Flames," Proc. Combustion Institute, Vol. 27, 1998, pp. 675-684.
13. Takahashi, F., and Katta, V. R., "A Reaction Kernel Hypothesis for the Stability Limit of Methane Jet Diffusion Flames," Proc. Combustion Institute, Vol. 28, 2000, pp. 2071-2078.
14. Katta, V. R., Takahashi, F., and Linteris, G. T., "Numerical Investigations of CO_2 as Fire Suppressing Agent," Fire Safety Science: Proceedings of the Seventh International Symposium, International Association for Fire Safety Science, 2003, pp. 531-544
15. Katta, V. R., Takahashi, F., and Linteris, G. T., "Suppression of Cup-Burner Flames Using Carbon Dioxide in Microgravity," Combustion and Flame 137, 506-522 (2004).
16. Linteris, G. T., Katta, V. R., and Takahashi, F., "Experimental and Numerical Evaluation of Metallic Compounds for Suppressing Cup-Burner Flames," Combustion and Flame 138, 78-96 (2004).
17. Katta, V. R., Takahashi, F., and Linteris, G. T., "Fire-Suppression Characteristics of CF_3H in a Cup Burner," Combustion and Flame, submitted (2004).
18. Takahashi, F., Linteris, G. T., and Katta, V. R., "Suppression of Cup-Burner Flames," Fourth International Symposium on Scale Modeling (ISSM-IV), Cleveland, OH, September 2003.
19. Takahashi, F., Linteris, G. T., and Katta, V. R., "Suppression Characteristics of Cup-Burner Flames In Low Gravity," AIAA-2004-0957, January 2004.
20. Takahashi, F., Linteris, G. T., and Katta, V. R., "Extinguishment of Cup-Burner Flames In Low Gravity," AIAA-2005-0711, Reno, NV, January 2005.
21. Roquemore, W. M., and Katta, V. R., "Role of Flow Visualization in the Development of UNICORN," Journal of Visualization, Vol. 2, No. 3/4, 257-272 (2000).
22. Frenklach, M., Wang, H., Goldenberg, M., Smith, G. P., Golden, D. M., Bowman, C. T., Hanson, R., K., Gardiner, W. C., and Lissianski, V., "GRI-Mech—An Optimized Detailed Chemical Reaction Mechanism for Methane Combustion," Technical Report No. GRI-95/0058, Gas Research Institute, Chicago, Illinois, 1995.
23. Anon., "NIST CKMech (Thermochemistry, Kinetics, Mechanisms)," http://fluid.nist.gov/ ckmech.html.
24. Annon., "Computational Submodels," International Workshop on Measurement and Computation of Turbulent Nonpremixed Flames., http://www.ca.sandia.gov/tdf/Workshop/ Submodels.html, 2001.
25. Katta, V. R., Goss, L. P., and Roquemore, W. M., "Numerical Investigatios of Transitional H_2/N_2 Jet Diffusion Flames," AIAA Journal 32: 84 (1994).
26. McBride, B. J., and Gordon, S., "Computer Program for Calculation of Complex Chemical Equilibrium Compositions and Applications—II. Users Manual and Program Description," NASA RP-1311, June 1996.
27. Warnatz, J., in *Combustion Chemistry* (W. C. Gardiner, ed.), Springer-Verlag, New York, 1984, pp. 197-360.